

# Determination of subcell I-V parameters by a pulsed suns-Voc method including optical coupling

H. Nesswetter,<sup>1</sup> N. R. Jost,<sup>1</sup> P. Lugli,<sup>2</sup> A. W. Bett,<sup>3</sup> and C. G. Zimmermann<sup>1</sup>

<sup>1</sup>Airbus DS, 81663 Munich, Germany

<sup>2</sup>Technical University of Munich, Arcisstr. 21, 80333 Munich, Germany

<sup>3</sup>Fraunhofer Institute for Solar Energy Systems ISE, Heidenhofstr. 2, 79110 Freiburg, Germany

(Received 7 December 2014; accepted 7 January 2015; published online 16 January 2015)

The open circuit voltage of a single subcell in a multijunction cell stack can be measured with the help of pulsed, millisecond illumination. This concept makes use of the fact that the charging of the non-illuminated cell capacitances takes place on a much longer timescale than of the illuminated one. Optical coupling introduces a photocurrent in the subcell underneath. Its efficiency can be quantified in parallel under short circuit conditions. A suns-Voc approach, applied to this subcell pair, yields all relevant diode parameters. Applied to all subcells of a Ga<sub>0.50</sub>In<sub>0.50</sub>P/Ga<sub>0.99</sub>In<sub>0.01</sub>As/Ge triple junction cell, a very good match to the dark I-V curve is obtained.

© 2015 AIP Publishing LLC. [<http://dx.doi.org/10.1063/1.4906237>]

Thermalization of electron hole pairs is the biggest loss mechanism in single junction solar cells. The stacking of subcells with different bandgaps on top of each other is currently the most successful concept to reduce these losses. Triple junction cells based on the material system Ga<sub>0.50</sub>In<sub>0.50</sub>P/Ga<sub>0.99</sub>In<sub>0.01</sub>As/Ge have reached efficiencies of 30% under the AM0 spectrum in space.<sup>1</sup> Under the concentrated terrestrial spectrum, record efficiencies of 44.7% have been reached in a wafer bonded GaInP/GaAs/GaInAsP/GaInAs four junction cell.<sup>2</sup> The characterization of individual subcells in such a multijunction solar cell, however, is complicated by the fact that only the series connected stack can be contacted externally. Recently, two methods have been proposed to circumvent this limitation. The first one makes use of Rau's reciprocity relation.<sup>3</sup> By measuring the electroluminescence spectrum of each subcell together with the external quantum efficiency (EQE), the open circuit voltage and subsequently the diode parameters of each subcell can be inferred.<sup>4</sup> The drawback of this method is that it requires high precision EQE measurement and, moreover, that it does not include optical coupling. In high quality III-V cells, a significant fraction of electron hole recombination is radiative. This radiation can be absorbed by the subcell underneath. This optical coupling effect, which introduces a voltage dependent current source, has been exploited to determine the ratio  $I_{01}/I_{02}$  of the dark saturation currents in individual subcells.<sup>5</sup> No absolute values, however, were obtained.

It is the purpose of this letter to introduce an alternative approach, based on a pulsed, monochromatic illumination of single subcells. Exploiting the non-negligible capacitance of all junctions, the open circuit voltage of the illuminated subcell can be measured during a millisecond pulse. With this tool to measure the subcell voltages, the diode parameters of all subcells can be extracted in a suns-Voc fashion.<sup>6</sup>

A 14.2 cm<sup>2</sup> Ga<sub>0.50</sub>In<sub>0.50</sub>P/Ga<sub>0.99</sub>In<sub>0.01</sub>As/Ge triple junction solar cell designed for space applications was chosen to verify this approach. To illuminate the three subcells independently, the electro- and photoluminescence setup

described in Ref. 7 was used. The top cell was illuminated homogeneously by a 405 nm LED array, whose radiation is completely absorbed there. A 803 nm and a 975 nm diode lasers were used for the external illumination of middle and bottom cells. Again photons of this wavelength are solely absorbed in the middle and bottom cells, respectively. The I-V curves were acquired at 300 K with a source-measure unit and 4-wire connections.

Starting with the bottom cell, Fig. 1(a) illustrates the time resolved open circuit voltage measured during a single 0.5 ms pulse of the 975 nm laser. The time resolution was 2  $\mu$ s and only the first pulse was measured to avoid additive charging effects by subsequent pulses. The typical capacitance of the single subcells is in the range of 1  $\mu$ F (Ref. 8), while the laser intensity for the depicted 975 nm pulse corresponds to a photocurrent of 0.331 A. Therefore, the bottom cell open circuit voltage is already built up after several  $\mu$ s.

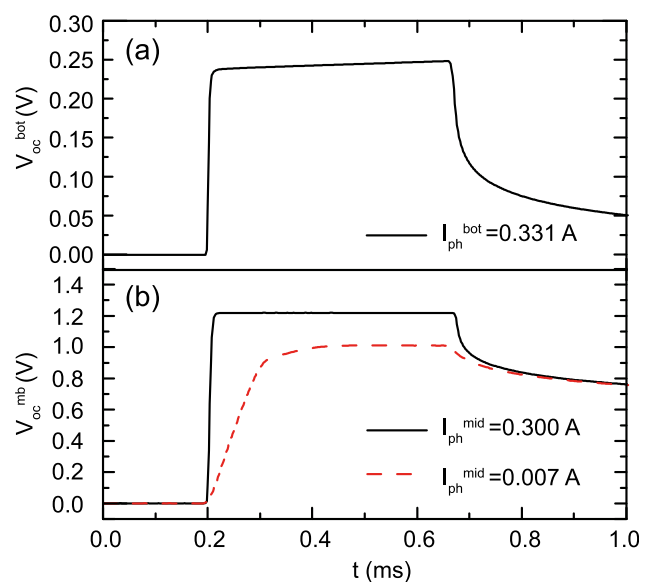


FIG. 1. Open circuit voltage of a triple junction cell during a 0.5 ms long pulse of (a) bottom cell illumination and (b) middle cell illumination. The corresponding photocurrents are indicated.

Next to this very fast rise time, which is in the same order of magnitude as the rise time of the laser intensity itself, an additional linear increase of the open circuit voltage is observed in Fig. 1(a). This can be attributed to parasitic absorption in the Ga<sub>0.99</sub>In<sub>0.01</sub>As middle cell due to impurities.<sup>9</sup> With the help of a Ga<sub>0.99</sub>In<sub>0.01</sub>As single-junction cell, it was verified that the 975 nm photons result in a photocurrent in the range of 10  $\mu$ A there. Since this photocurrent is orders of magnitude smaller than the photocurrent of the bottom cell under external illumination, the build up of an open circuit voltage in the middle cell takes place on a much longer timescale.

At the end of the 0.5 ms laser pulse, a contribution of about 10 mV from the middle cell results, but at the beginning of the plateau it is well below 1 mV and thus can be neglected. For lower intensities of the 975 nm laser, this effect is even less pronounced. A bottom cell open circuit voltage  $V_{oc}^{bot}$  of 0.238 V is derived from Fig. 1(a) at this point in time. The photocurrent generated in bottom and middle cells, together with the external measurement circuit, results in a charging and the build up of a voltage of opposite polarity in the top cell. The measurement device has an internal resistance  $R$  of 1 M $\Omega$ . Combined with the top cell capacitance  $C$  around 1  $\mu$ F, this leads to an RC time constant of 1 s. Therefore, even at the end of the pulse, a negligible voltage drop below 1 mV at the top cell is found. It has to be noted that without parasitic absorption in the middle cell, the same approach is valid, with the combined capacitance of top and middle cells taking the role of the top cell capacitance. After the switch off of the illumination, an exponential decay takes over.

In high quality multijunction cells, it is justified to neglect shunt and series resistance effects. All subcells can thus be modeled by a simple two diode model, with parameters  $I_{01}$  and  $I_{02}$ . Under open circuit conditions, the following equation holds for the bottom cell:

$$I_{ph}^{bot} = I_{01}^{bot} e^{\left(\frac{qV_{oc}^{bot}}{kT}\right)} + I_{02}^{bot} e^{\left(\frac{qV_{oc}^{bot}}{2kT}\right)}. \quad (1)$$

The photocurrent of the bottom cell is denoted by  $I_{ph}^{bot}$  and  $q$ ,  $k$ , and  $T$  have their usual meaning. By measuring  $V_{oc}^{bot}$  for different photocurrents  $I_{ph}^{bot}$ , which can be generated by different laser pulses,  $I_{01}^{bot}$  and  $I_{02}^{bot}$  can be extracted from a fit to the suns-Voc curve according to Eq. (1).

The correlation between laser intensity  $\Phi_{bot}$  and photocurrent  $I_{ph}^{bot}$  for the bottom cell as well as for the remaining junctions can be determined by several approaches. Component cells, i.e., cells without activated top and middle cells, could be used. Alternatively, the photocurrent could be determined with the help of the measured EQE of the subcells. The approach chosen here was aiming at an experimentally simpler, yet equally precise determination. It requires steady state laser illumination. With the help of a Si photodiode, it was verified that the steady state and pulsed laser intensities for a given laser power setting were identical. Middle and bottom cells are first illuminated with an intensity at the upper end of the available range. The short circuit current  $I_{sc}$  of the complete cell is measured while increasing the top cell illumination  $\Phi_{top}$ ,<sup>10</sup> starting from zero

illumination. At a certain intensity setting,  $I_{sc}$  will no longer increase linearly with  $\Phi_{top}$ , but only indirectly due to optical coupling contributions into the other junctions. Up to this cross-over point, the top cell is the limiting subcell and the  $I_{ph}^{top}/\Phi_{top}$  correlation can be obtained straightforwardly. For the middle cell, the top cell illumination is first set to the desired  $I_{ph}^{mid}$  value to be calibrated, and the bottom cell remains over-illuminated as before. The middle cell illumination is then increased from zero until  $I_{sc}$  does not change anymore. At this point, top and middle cells are current matched and the measured  $I_{ph}^{mid}$  can be correlated to  $\Phi_{mid}$ . In case of the bottom cell, top and middle cells are illuminated in the current matched conditions just determined.  $\Phi_{bot}$  is increased, again until  $I_{sc}$  remains constant. Then, all three junctions are current matched and  $I_{ph}^{bot}$ , which equals  $I_{ph}^{mid}$ , can be related to the bottom cell illumination level. As outlined in more detail later, the current matched conditions ensure that optical coupling contributions to the measured photocurrent from junctions higher up are negligible. Consequently, the entire procedure has to be repeated, if other illumination levels are to be calibrated for middle and bottom cells.

In Fig. 2(a), the resulting suns-Voc data points and the fit according to Eq. (1) are plotted. ( $I_{01}^{bot}$ ,  $I_{02}^{bot}$ ) are obtained as ( $3.1 \times 10^{-5}$  A,  $7.3 \times 10^{-5}$  A). Moving upwards in the cell stack, only the middle cell is illuminated with the 803 nm laser by a 0.5 ms pulse which generates a certain photocurrent  $I_{ph}^{mid}$ . Optical coupling introduces a photocurrent in the bottom cell as well and only the combined open circuit voltage  $V_{oc}^{mb}$  of the middle and bottom subcells is measured. In the measurement shown in Fig. 1(b), the laser intensity corresponds to a photocurrent  $I_{ph}^{mid}$  of 0.300 A in the middle cell. In high quality triple junction cells, the optical coupling from middle to bottom cell is high and such both cells are charged within  $\mu$ s. The charging of the top cell takes place on a much longer timescale, as argued above, and is not visible in this diagram. In cells with low optical coupling efficiency or at much lower illumination intensity, the difference in charging time constants in bottom and middle cells becomes visible, as shown in Fig. 1(b) for a  $I_{ph}^{mid}$  of 7 mA. But even in this case, the plateau is reached well within the 0.5 ms pulse.

The situation of the middle cell is thus described in analogy to Eq. (1),

$$I_{ph}^{mid} = I_{01}^{mid} e^{\left(\frac{qV_{oc}^{mid}}{kT}\right)} + I_{02}^{mid} e^{\left(\frac{qV_{oc}^{mid}}{2kT}\right)}. \quad (2)$$

The illumination of the bottom cell is solely governed by the optical coupling current, which is proportional to the current through diode 1 in the middle cell.<sup>5</sup> The proportionality constant is the coupling efficiency  $\eta_{mb}$ ,

$$\eta_{mb} I_{01}^{mid} e^{\left(\frac{qV_{oc}^{mid}}{kT}\right)} = I_{01}^{bot} e^{\left(\frac{qV_{oc}^{bot}}{kT}\right)} + I_{02}^{bot} e^{\left(\frac{qV_{oc}^{bot}}{2kT}\right)}, \quad (3)$$

and the measured open circuit voltage  $V_{oc}^{mb}$  is the sum of the middle cell open circuit voltage  $V_{oc}^{mid}$  and  $V_{oc}^{bot}$ ,

$$V_{oc}^{mb} = V_{oc}^{bot} + V_{oc}^{mid}. \quad (4)$$

Combining Eqs. (2)–(4) and solving for  $V_{oc}^{mb}$  yield

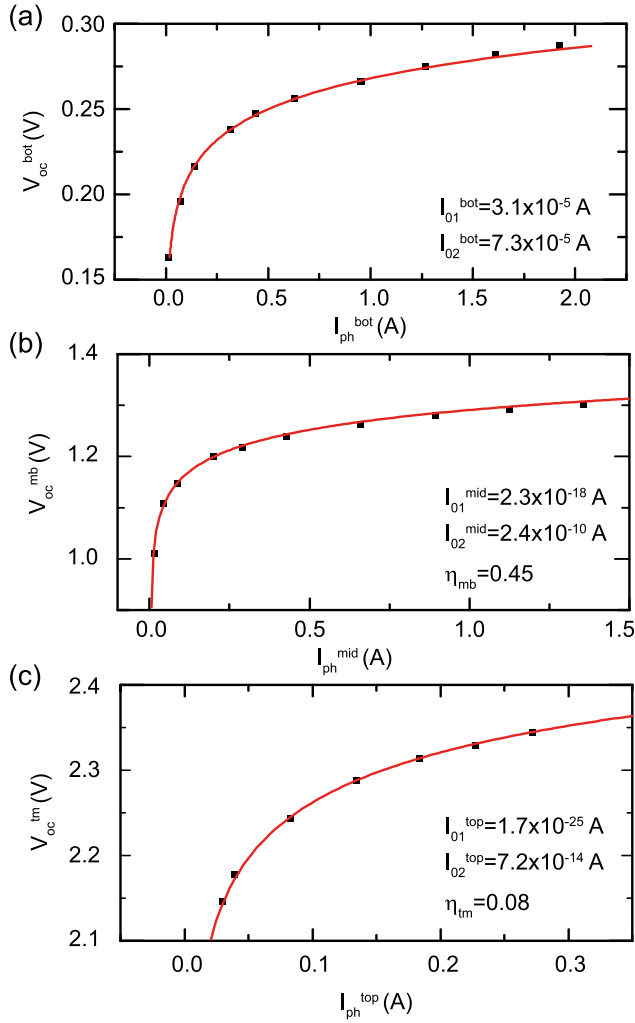


FIG. 2. Open circuit voltage-photocurrent dependence measured for (a) the bottom cell, (b) the middle-bottom cell pair, and (c) the top-middle cell pair. The corresponding fits according to Eqs. (1) and (5) and the subcell parameters derived are also included.

$$e \left( \frac{qV_{oc}^{mb}}{2kT} \right) = \frac{\sqrt{I_{ph}^{mid} + \phi_{mid}^2} - \phi_{mid}}{\sqrt{I_{01}^{bot} I_{01}^{mid}}} \times \left( \sqrt{\phi_{bot}^2 + \eta_{mb} \left( \sqrt{I_{ph}^{mid} + \phi_{mid}^2} - \phi_{mid} \right)^2} - \phi_{bot} \right). \quad (5)$$

$\phi_{mid}$  and  $\phi_{bot}$  denote the ratio  $I_{02}/2\sqrt{I_{01}}$ , for middle and bottom cells, respectively. Equation (5) is the basis to fit the middle cell suns- $V_{oc}$  curve to the measured  $V_{oc}^{mb}-I_{ph}^{mid}$  data. What is required in addition is the illumination level of the bottom cell as governed by  $\eta_{mb}$ . In Eq. (5), the unknown parameters  $I_{01}^{mid}$  and  $\eta_{mb}$  are not independent. This is easily verified for the special case of  $\phi_{mid} = \phi_{bot} = 0$ . Thus,  $\eta_{mb}$  is determined by an additional steady state measurement under short circuit conditions through the approach suggested by Steiner and Geisz.<sup>5</sup>

In this case, top and middle cells are illuminated constantly and  $I_{sc}$  of the cell is measured. Since the bottom cell is not illuminated externally,  $I_{sc}$  corresponds to the optical coupling current from middle to bottom cell,  $I_{mb}$ . Neglecting

the effect of the top cell for the moment, this optical coupling current is a function of the available recombination current  $I_{ph}^{mid} - I_{mb}$  in the cell.<sup>5</sup> Steiner and Geisz derived the following functional dependence:

$$I_{mb} = \eta_{mb} \left( \sqrt{I_{ph}^{mid} - I_{mb} + \phi_{mid}^2} - \phi_{mid} \right)^2. \quad (6)$$

The influence of the top cell complicates things. Optical coupling from top to middle cell increases the current in the middle cell and thus  $I_{mb}$ . The amount of optical coupling from top to middle cell, however, depends on the available recombination current in the top cell and thus again on the difference  $I_{ph}^{top}$  and  $I_{mb}$ . This leads to an implicit equation which involves the optical coupling parameters of all subcells.<sup>5</sup>

In the context of this work, we suggest measurement conditions to eliminate the influence of the top cell. For a constant middle cell illumination,  $I_{mb}$  is measured as a function of the top cell illumination level. Decreasing the top cell illumination will gradually decrease  $I_{mb}$  as the optical coupling contribution in the middle cell decreases. At a certain point,  $I_{mb}$  will decrease linearly with the top cell illumination. At the cross-over point between these two different slopes,  $I_{ph}^{top}$  exactly matches  $I_{mb}$  and there is no top cell influence any more. Equation (6) is then valid exactly. The same approach is also valid in N-junction solar cells, as only the illuminated and the two neighboring junctions are to be considered.

Combining Eqs. (5) and (6) yields the final fit equation

$$e \left( \frac{qV_{oc}^{mb}}{2kT} \right) = \frac{\sqrt{I_{ph}^{mid} + \phi_{mid}^2} - \phi_{mid}}{\sqrt{I_{01}^{bot} I_{01}^{mid}}} \times \left( \sqrt{\phi_{bot}^2 + \frac{I_{mb} \left( \sqrt{I_{ph}^{mid} + \phi_{mid}^2} - \phi_{mid} \right)^2}{\left( \sqrt{I_{ph}^{mid} - I_{mb} + \phi_{mid}^2} - \phi_{mid} \right)^2}} - \phi_{bot} \right). \quad (7)$$

For every given middle cell photocurrent  $I_{ph}^{mid}$ , the corresponding  $V_{oc}^{mb}$  is measured pulsed under open circuit conditions and  $I_{mb}$  is measured steady state under short circuit conditions. By minimizing the quadratic differences between the measurements and Eq. (7),  $I_{01}^{mid}$ ,  $\phi_{mid}$ , and thus also  $I_{02}^{mid}$  are obtained. Based on Eq. (6),  $\eta_{mb}$  is subsequently derived. For the cell analyzed here, the middle cell parameters ( $I_{01}^{mid}$ ,  $I_{02}^{mid}$ ,  $\eta_{mb}$ ) were determined to ( $2.3 \times 10^{-18}$  A,  $2.4 \times 10^{-10}$  A, 0.45). In Fig. 2(b), the functional dependence of  $V_{oc}^{mb}$  on  $I_{ph}^{mid}$  according to Eq. (5) is plotted, together with the measured data points.

For the top cell, the same procedure and the same equations can be applied analogously. In order to still limit the analysis under open circuit conditions to the illuminated subcell and the subcell underneath, the bottom cell in this case is over-illuminated very strongly. Thus, any optical coupling contribution into the bottom cell is negligible and its open circuit voltage remains constant. With the help of the bottom

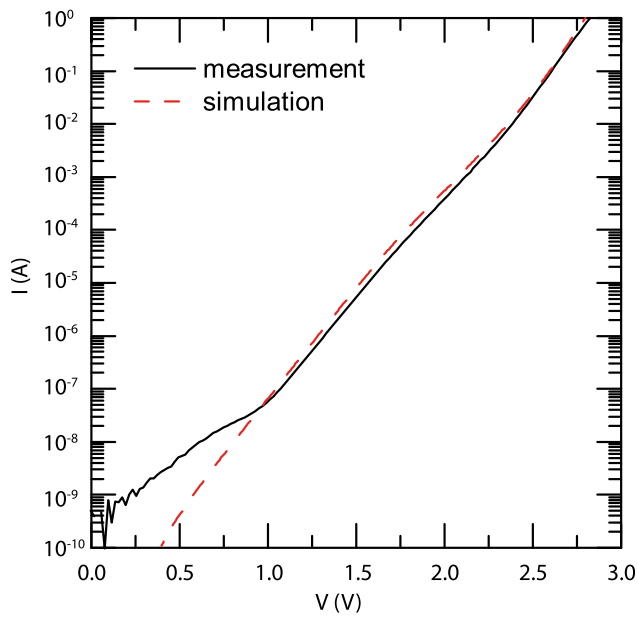


FIG. 3. Dark I-V curve simulated based on the diode parameters determined for the different subcells. A very good match to the measured dark I-V curve is obtained.

cell parameters already determined,  $V_{oc}^{bot}$  can be calculated and eliminated from the measurement. Likewise, an over-illuminated bottom cell in the determination of the coupling efficiency between top and middle cell,  $\eta_{tm}$ , limits the analysis under short circuit conditions to the top/middle subcell pair. Analysis of the uppermost junction has the additional benefit that the combined open circuit voltage  $V_{oc}^{tm}$  of top and middle cells can be measured under steady state conditions, since all junctions are either illuminated directly or through optical coupling. The top cell parameters ( $I_{01}^{top}$ ,  $I_{02}^{top}$ ,  $\eta_{tm}$ ) were derived as ( $1.7 \times 10^{-25}$  A,  $7.2 \times 10^{-14}$  A, 0.08). In Fig. 2(c), the measured data points and the  $V_{oc}^{tm} - I_{ph}^{top}$  fit are illustrated.

As independent verification, the dark I-V characteristic of the cell analyzed was measured. In parallel, the dark I-V curve was modeled. To conveniently take into account also the optical coupling parameters, a simulation program with integrated circuit emphasis (SPICE) was used. Although only having a small impact on the dark I-V curve at high voltages, in this framework the optical coupling contributions could be modeled straightforward as arbitrary behavioral current sources. For the diode elements, the experimentally determined diode parameters were used. As shown in Fig. 3, a remarkable agreement is obtained which confirms the validity of the method. The deviation for very low currents is caused by shunts, which could not be taken into account in the simulation.

In conclusion, all subcell parameters in a multijunction solar cell stack, including the optical coupling parameters, can be determined with the help of the pulsed illumination method. The analysis is only based on pairs of two adjoining

subcells and can thus be easily extended from the triple junction cell example presented here to a cell stack with any number of junctions. The pulsed illumination method relies on the fact that the charging time of the directly and optical coupling illuminated subcells is orders of magnitude faster than the subsequent charging of the non-illuminated subcells. The latter is only limited by the internal resistance of the measurement equipment used and was three orders of magnitude larger in the setup used here, even for the lowest illumination currents. For scenarios in which the optical coupling is severely reduced, for example, if the evolution of the subcell parameters during a particle radiation campaign is to be followed, the same procedure could still be used, merely the pulse duration has to be extended. In this case, there is a pronounced difference between the rise time of the directly illuminated subcell and the subcell illuminated via optical coupling. This can be used to determine the open circuit voltage of the illuminated cell directly, which simplifies the procedure.

The applicability of the pulsed suns-Voc method is only limited by the presence of shunts in the directly or optical coupling illuminated subcells. A shunt in the 1000  $\Omega$  range discharges the illuminated cells with a ms time constant, which is in the same order of magnitude as the pulse duration. For high illumination conditions, resulting in 10 mA/cm<sup>2</sup> photocurrents, the charging of the capacitance is still significantly faster, but for low illumination conditions in the 0.1 mA/cm<sup>2</sup> range, which is especially relevant in the cell only illuminated by optical coupling, the actual open circuit voltage can only be extrapolated based on a fit of the discharge curve. Severely shunted cells below 100  $\Omega$  shunt resistance are beyond the scope of this method.

<sup>1</sup>A. W. Bett, S. P. Philipps, S. Essig, S. Heckelmann, R. Kellenbenz, V. Klinger, M. Niemeyer, D. Lackner, and F. Dimroth, in *Proceedings of the 28th European Photovoltaic Specialist Conference* (WIP, Munich, Germany, 2013), pp. 1–6.

<sup>2</sup>F. Dimroth, M. Grave, P. Beutel, U. Fiedeler, C. Karcher, T. N. D. Tibbits, E. Oliva, G. Siefert, M. Schachtner, A. Wekeli, A. W. Bett, R. Krause, M. Piccin, N. Blanc, C. Drazek, E. Guiot, B. Ghyselen, T. Salvat, A. Tauzin, T. Signamarcheix, A. Dobrich, T. Hannappel, and K. Schwarzburg, *Prog. Photovoltaics* **22**, 277 (2014).

<sup>3</sup>U. Rau, *Phys. Rev. B* **76**, 085303 (2007).

<sup>4</sup>S. Roensch, R. Hoheisel, F. Dimroth, and A. W. Bett, *Appl. Phys. Lett.* **98**, 251113 (2011).

<sup>5</sup>M. A. Steiner and J. F. Geisz, *Appl. Phys. Lett.* **100**, 251106 (2012).

<sup>6</sup>M. Wolf and H. Rauschenbach, *Adv. Energy Convers.* **3**, 455 (1963).

<sup>7</sup>H. Nesswetter, P. Lugli, A. W. Bett, and C. G. Zimmermann, *IEEE J. Photovoltaics* **3**, 353 (2013).

<sup>8</sup>In a rough approximation, the junction capacitance  $C$  is derived as  $C = A \sqrt{\frac{\epsilon_0 \epsilon_r q N_A N_D}{2(N_A + N_D) U_D}} \approx 1 \mu\text{F}$ , with  $A = 14.2 \text{ cm}^2$ ,  $\epsilon_0 \epsilon_r \approx 10^{-10} \text{ F/m}$ ,  $N_A \approx 10^{17} \text{ cm}^{-3}$ ,  $N_D \approx 10^{18} \text{ cm}^{-3}$ , and  $U_D \approx 1 \text{ V}$ , which is in the range of values measured experimentally.

<sup>9</sup>M. Sturge, *Phys. Rev.* **127**, 768 (1962).

<sup>10</sup>In case of a non ideal reverse characteristic, the cell current can be read out on the IV curve at  $V_{oc} - V_{oc}^{subcell}$ , where  $V_{oc}^{subcell}$  denotes the expected open circuit voltage of the limiting subcell.